Engenharia Agrícola

ISSN: 1809-4430 (on-line)

www.engenhariaagricola.org.br

Scientific Paper
Doi: http://dx.doi.org/10.1590/1809-4430-Eng.Agric.v44e20230087/2024

OPTIMIZATION AND TEST OF THE OPERATING PARAMETERS OF A *CAMELLIA OLEIFERA* FRUIT PICKING DEVICE UNDER THE SYNERGISTIC ACTION OF A VIBRATION COMB

Cheng Wu[1], Rongyan Wang[1], Junhua Yang[1], Dong Fang[1], Delin Wu[1*]

[1*]Corresponding author. School of Engineering, Anhui Agricultural University, Hefei 230036, China.
E-mail: wudelin@126.com | ORCID ID: https://orcid.org/0000-0001-9839-6354

KEYWORDS

Camellia fruit, vibration-comb type, rigid-flexible coupled, Adams, performance test.

ABSTRACT

There are significant differences in the quantities of *Camellia oleifera* fruits growing within and outside the canopy distribution, meaning that a single mode of picking has drawbacks. To improve the harvesting efficiency for the inner and outer layers, this article proposes a synergistic mode of harvesting based on a vibration comb brush, and presents a design for a harvesting device based on this principle. The overall structure and working principle of the proposed device are explained, and the operational processes of the vibration and comb parts of the device are analyzed. ADAMS software is used to construct a rigid-flexible coupling model of the device and the fruiting branch, and simulation results are presented to show that the fruit drop and flower loss rates for *Camellia oleifera* are related to the vibration frequency, the amplitude, and the spacing between the teeth and comb plates. Finally, a three factor and three level field orthogonal experiment was conducted, and the results showed that under the conditions of vibration frequency 5.85Hz, amplitude 60.43mm, and comb spacing 45mm, the flower loss rate was the lowest and it had good picking performance. Under these conditions, the fruit drop rate is 87.32% and the flower loss rate is 8.06%, values that meet the requirements for mechanized picking of *Camellia oleifera* fruits.

INTRODUCTION

Camellia oleifera is a high-yield oil crop that is widely cultivated in China. It is rich in saponins, with hemolytic, antibacterial, and industrial uses (Zhu et al., 2023), and is preferred by the World Food and Agriculture Organization as a raw material for healthy edible oil. Today, the mechanized picking of *C. oleifera* fruits has become a development trend in the fruit industry; a method based on an end effector is mainly used for picking, and is more common than in other fruit-picking applications. For example, Yu et al. (2023) used vibration to harvest *Coffea arabica L.*; He et al. (2022) used a double robotic arm to automatically pick kiwifruit, with significantly effective results; and Hayashi et al. (2014) developed a strawberry picking end effector to improve the efficiency of strawberry picking.

In existing research, vibration or brushing methods have mainly been used for picking *C. oleifera* fruits. Gao et al. (2019) designed a suspension-vibration-type actuator for picking *C. oleifera* fruit in which mechanical vibration was applied to the main trunk of the fruit tree, producing forced vibration and driving the fruit to undergo accelerated movement. The movement of the fruit generated by the inertial force was greater than the fruit and branch combination force, meaning that the fruit fell from the tree. Wang et al. (2020) designed a vibration-type harvesting machine for green *C. oleifera* fruit in which a vibrator crank linkage design was adopted. The circular motion of the crank drove the telescopic rod to undergo reciprocating linear motion, thereby producing a vibration excitation force that forced the fruit to detach. Wu et al. (2022) developed a canopy-vibration-type machine for picking *C. oleifera* fruit, which improved the efficiency of fruit shedding by applying an effect based on the optimal excitation point of the canopy branches.

Comb picking has also been reported in the literature. Gao et al. (2013) developed a tooth-comb-type machine for

[1] School of Engineering, Anhui Agricultural University, Hefei 230036, China.

Area Editor: Murilo Mesquita Baesso
Received in: 6-13-2023
Accepted in: 5-27-2024

picking *C. oleifera* fruit in which rotary comb teeth were used to produce a shear force on the fruit, and which achieved high efficiency in terms of fruit picking. Luo et al. (2017) developed a device based on a tooth comb and paddle knife for picking *C. oleifera* fruit, where the paddle knife produced tension on the fruit to achieve harvesting. Rao et al. (2018) designed a device with a rotating electric rubber roller for picking *C. oleifera* fruit; through the impact of the upper and lower rubber rollers on the fruit, a pull force was produced that was greater than the combination force on the fruit, thereby achieving picking. Wu et al. (2021b) developed an end effector in which a twisted comb was used for picking *C. oleifera* fruit. This device exerted a variety of forces on the fruit that caused it to fall off.

However, despite the markedly uneven distribution of the numbers of *C. oleifera* fruit growing inside and outside of the canopy (Du et al., 2022), most existing picking equipment is based on a single mode, and there would be significant advantages from the development of a multi-mode cooperative form of operation for picking the inner and outer fruits. In this paper, a vibration-comb picking device is designed based on an analysis of the vibration and comb picking processes; the proposed device vibrates and collides with the outer layer of *C. oleifera* fruit while rotating and combing the inner layer. The development of a multi-mode device for picking *C. oleifera* fruit will have long-term importance for the efficiency of mechanized picking of this crop.

MATERIAL AND METHODS

Analysis of the Vibration Process of *Camellia Oleifera* Fruit

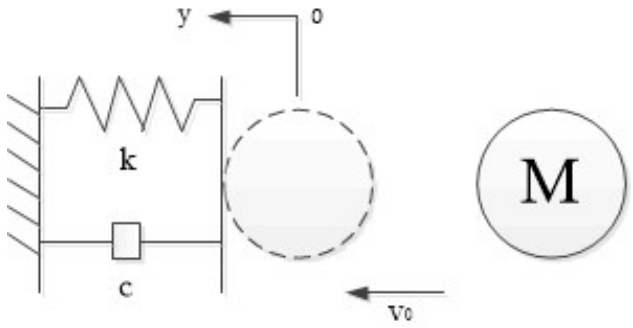

FIGURE 1. Fruit-vibrator collision model.

Under collisional contact between the oleaginous fruit and the vibration device (Fu et al., 2020), the motion satisfies the following equations:

$$M\frac{d^2y}{dt^2}+c\frac{dy}{dt}+ky=0 \tag{1}$$

$$y(0)=0 \tag{2}$$

$$y'(0)=v_0 \tag{3}$$

in which

M - mass of the Camellia oleifera fruit before the collision, kg;

c - damping factor of the vibrating rod, N·s/m;

k - stiffness of the vibrating rod, N/m;

v_0 - initial velocity of the vibrating rod when it collides with the fruit, m/s.

The solution to the above equations in the under-damped case is

$$y(t)=Ae^{-\xi\omega nt}\sin(\omega_d t) \tag{4}$$

$$\xi=\frac{c}{2M\omega_n} \tag{5}$$

$$A=\frac{v_0}{\omega} \tag{6}$$

$$\omega_d=\sqrt{1-\xi^2}\omega_n \tag{7}$$

$$\omega_n=\sqrt{k/M} \tag{8}$$

in which

A - amplitude of the vibrating plate, mm;

$y(t)$ - displacement of the oleander, mm;

ξ - viscous damping ratio, $\xi<1$;

ω_d - damped inherent frequency, Hz;

ω_n - undamped natural frequency, Hz.

Due to the zero force on the fruit at the beginning and end of the collision, it can be concluded:

$$y''(t)=0 \tag{9}$$

Substituting [eq. (9)] into [eq. (4)] gives

$$-Ae^{-\xi\omega nt}[(1-2\xi^2)\omega_n\sin(\omega_d t)+2\xi\omega_d\cos(\omega_d t)]=0 \tag{10}$$

The two solutions to [eq. (10)] are t_0 and t_1, where t_0 = 0 and the minimum positive solution t_1 is the collision time

$$\Delta t = t_1 = \frac{\pi - rac\tan\lambda_1}{\omega_n\sqrt{1-\xi^2}} \tag{11}$$

in which

$$\lambda_1 = \frac{2\xi\sqrt{1-\xi^2}}{1-2\xi^2} \tag{12}$$

From eqs (11) and (12), it can be concluded that the operating time for the picking actuator is equal to the duration of the collision with the *C. oleifera* fruit, which is directly related to the natural frequency and viscous damping ratio of the actuator vibration source.

Force Analysis of the Comb Teeth on the Fruit

Figure 2 shows a sketch of the forces applied to the *C. oleifera* fruit during picking by the toothed comb plate.

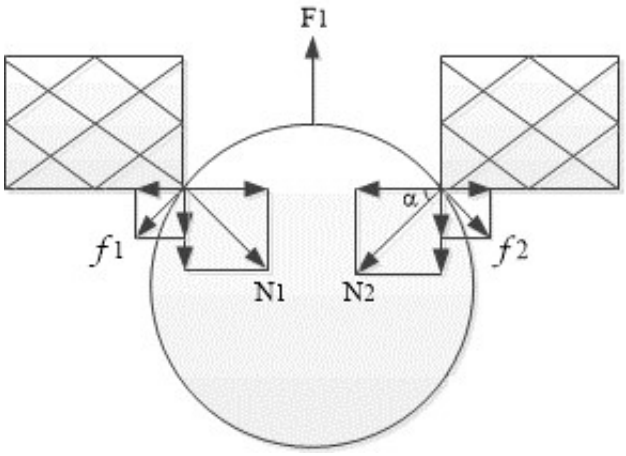

FIGURE 2. Map of stresses exerted on the fruit under combing action.

$$f_1 = \mu N_1 \tag{13}$$

$$f_2 = \mu N_2 \tag{14}$$

$$F_X = N_1\cos\alpha - N_2\cos\alpha - f_1\sin\alpha + f_2\sin\alpha \tag{15}$$

in which

f_1, f_2 - friction in the direction tangential to the fruit during the combing operation, N;

N_1, N_2 - positive pressure on the fruit during the carding operation, N;

F_X - division of the combined force on the fruit by the comb teeth along the horizontal direction, N.

From eqs (13), (14) and (15), we see that the mechanical condition for the abscission of the *C. oleifera* fruit is as follows:

$$F_1 \le (N_1 + N_2)\sin\alpha + \mu\cos\alpha(N_1 + N_2) \tag{16}$$

Based on the above analysis, it can be seen that during the operation of the picking device, factors such as the vibration frequency and amplitude of the vibrating rod, the spacing between the comb plates, and the operating time will affect the shedding of oil fruits. It is also related to the quality of the fruit itself, the binding force of the stem, and the material characteristics of the picking device. Based on the study of two harvesting modes, structural design and simulation analysis were carried out.

Design of a Vibration-Comb-Type C. Oleifera Fruit Picking Device

Based on our analysis of two picking modes, a fruit picking device is designed that can apply vibration and brushing functions simultaneously. It mainly consists of a power source, transmission device, connecting device, and picking actuator. The picking actuator includes a vibration mechanism and a comb brush mechanism, which are connected via a double plate connection frame. The entire picking actuator is fixed on a lifting platform, and the lifting platform and support frame are fixed to a mobile device. A schematic diagram of the structure of the picking device is shown in Figure 3. During the picking process, the device combines the vibration effect of the vibrating plate with the stripping effect of the toothed comb plate. The outer layers of *C. oleifera* fruits are picked by vibration, while the inner layers of fruits are stripped from the plant.

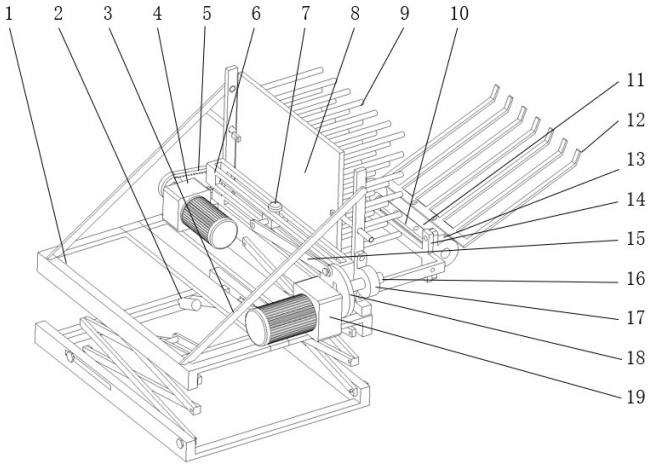

FIGURE 3. Structure of the proposed picking device: (1) lifting platform; (2) electric push rod; (3) vibration plate frame; (4) electric motor I; (5) transmission belt; (6) vibration plate frame; (7) slider limit pin; (8) vibration plate; (9) vibration rod; (10) tooth comb transmission shaft; (11) tooth comb connecting plate; (12) tooth comb plate; (13) bearing with seat I; (14) double plate connecting frame; (15) connecting rod; (16) vibration transmission shaft; (17) bearing with seat II; (18) eccentric disk; (19) motor II.

Table 1 shows the specific performance parameters of the device. During operation, the picking device moves to the canopy area of the *C. oleifera* tree, and the upper part of the picking device is inserted into the canopy with the fruit.

Motor I is started and transmits power to the eccentric disk through the vibration transmission shaft. The rotation of the eccentric disk drives the slider on the connecting rod to pull the vibration plate, causing the vibration plate to move horizontally and reciprocally in the chute. The vibration rod installed on the vibration plate collides, strikes, and clamps the disorderly distribution of *C. oleifera* fruits, causing them to separate and fall from the branches. At this point, the vibrating rod will also exert vibration on the branches, forcing the fruit to fall off under the centrifugal force. Due to the toughness of the branches and their contact with the flexible material of the nylon vibrating rod, this short-term action will not cause excessive damage to them. Motor II, which is started at the same time, drives the tooth comb transmission shaft to rotate via the transmission belt, causing the tooth comb plate installed on the tooth comb transmission shaft to rotate slowly within the range 0–90°. It combs and brushes the fruit, and causes it to fall under force. The rotation path of the tooth comb plate conforms to the biological curve of the fruiting *C. oleifera* branch, following the bent and deformed shape of the branch. Finally, the entire device is extracted from the canopy, and the toothed comb plate exerts a secondary effect on the surface of the canopy until the entire extraction process is completed. During the vibration and brushing operations, the fruit will be subjected to different forms of force, ensuring a high fruit drop rate. Due to the large spacing between the vibration rod and the tooth comb plate and the use of a flexible nylon material, any flower buds in the gap between the vibration rod and the tooth comb will be missed, and damage to the branches will be reduced.

TABLE 1. Performance parameters for the complete machine.

Serial number	Performance parameter	Numerical value
1	Working area (mm)	500×360×240
2	Picking height (mm)	1200–2000
3	Tooth comb spacing (mm)	25, 30, 35
4	Vibrating rod length (mm)	200
5	Vibrating rod arrangement	6×7
6	Vibrating rod spacing (mm)	45
7	Motor power (W)	120
8	Motor speed range (r/min)	1400–2800
9	Vibrating plate sliding range (mm)	0–80

The horizontal reciprocating motion of the vibrating rod is based on the use of the crank slider mechanism to convert circular motion into linear motion. The simple harmonic force generated by the horizontal reciprocating motion of the vibrating rod is used as the excitation and collision force for the vibration of the fruit. A motion diagram is shown in Figure 4.

From an analysis of Figure 4, showing that the displacement equation for the motion of the vibrating plate is:

$$X = r\cos\omega t \tag{17}$$

Further equations can be obtained as follows:

$$v = -\omega r\sin\omega t \tag{18}$$

$$\alpha = -\omega^2 r\cos\omega t \tag{19}$$

$$F = -m\omega^2 r\sin\omega t \tag{20}$$

in which

X - displacement of the vibrating plate, m;

r - eccentricity, m;

v - angular velocity of the eccentric disk, m/s;

α - acceleration of the vibrating plate, m/s^2;

F - reciprocating force, N.

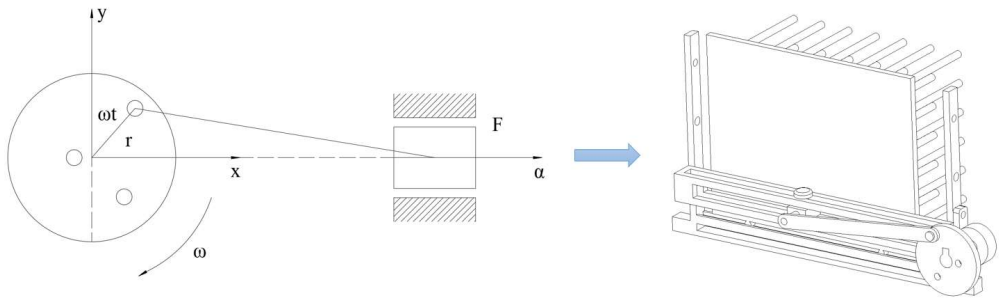

FIGURE 4. Diagram showing the principle of operation of the vibrating rod.

The rotary motion of the toothed comb plate is used to pick the inner layer of *C. oleifera* fruit. Consider the characteristics of the plant and an analysis of the dynamic characteristics of the toothed comb plate during its operation in order to reduce damage to flower buds and branches during movement, and a diagram of the motion is shown in Figure 6, where $O_0X_0Y_0$ is the inertial coordinate system, OXY is the dynamic coordinate system of the flexible tooth comb plate and the deformation movement fixed to the O point of the tooth comb transmission shaft. A_1 rotates around the point O_0 on a fixed axis, and the flexible tooth comb plate A_1 rotates in the plane $O_0X_0Y_0$, extends along the axis OX, and undergoes deformation. Q refers to any point on the extended flexible tooth comb plate; in the undeformed state of the flexible tooth comb plate, the coordinates of point Q in the dynamic coordinate system are (x, 0), whereas in the deformed state, the coordinates are (X (x, t), Y (x, t)).

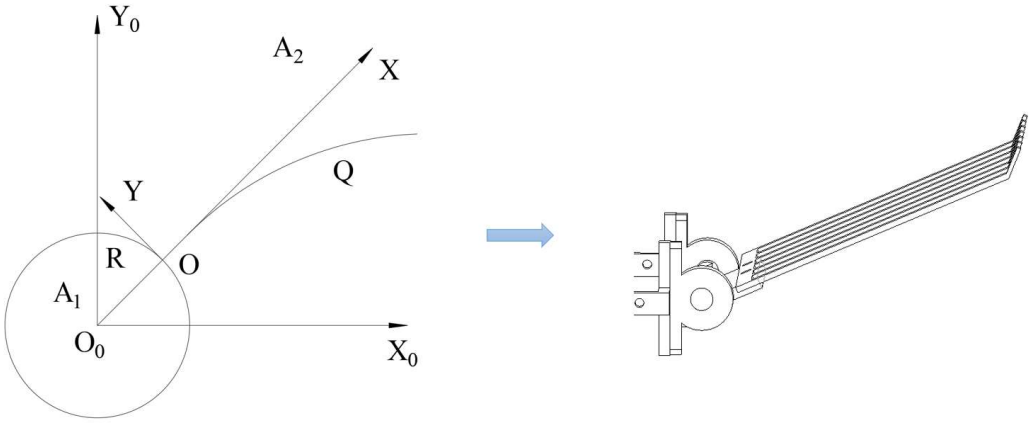

FIGURE 5. Schematic diagram showing the motion of the tooth comb plate.

Expressions for the radial direction (r) , velocity (V), acceleration (A) , and moment of momentum at point Q are as follows:

$$r = [R + X(x,t)]i + Y(x,t)\,j \tag{21}$$

$$V = (X' - Y'\alpha)i + [Y' + (R + r)\alpha']j \tag{22}$$

$$A = [x'' - 2Y'\alpha' - Y\alpha'' - (R + x)\alpha'']i + [Y'' + 2x'\alpha' + (R + r)\alpha'' - Y\alpha'']j \tag{23}$$

The moment of momentum of the flexible tooth comb plate around the tooth comb transmission shaft is then:

$$G = Ri \times (M_i - \rho AL)\frac{d(Ri)}{dt} + \rho A\int_0^L r \times r'dx \tag{24}$$

$$= R^2(M_1 - \rho AL)\alpha' k + \rho A\int_0^L \{(R + x)[Y' + (R + x)\alpha'] - Y(x' - Y\alpha')\}dxk \tag{25}$$

in which

A_1 - gear comb plate transmission shaft;

A_2 - flexible tooth comb plate;

L (t) - length of the extended flexible tooth comb plate in the OX direction without deformation;

O - accumulation point of the flexible tooth comb plate without extension;

i - unit vector for the OX axis;

j - the unit vector for the OY axis.

Kinematics Simulation

A simulation was carried out using ADAMS simulation software, which allows for the rigid-flexible coupling of the picking device and the branch to be simulated. We used variable control methods to simulate and analyze multiple parameters simultaneously, to obtain the response of the branches under different operating parameters (Li et al., 2015).

The picking device is in direct contact with the *C. oleifera* branch and fruit during the process, and is a rigid body, while the fruiting branch is a flexible body. Hence, in the simulation process, the branches need to be flexibly processed to ensure the accuracy of the simulation data (Zhang et al., 2018; Yu et al., 2021). The workflow for this simulation was as follows:

(1) Addition of constraints: When the flexible body generated to represent the fruit-bearing branch has been imported into ADAMS, the corresponding constraints need to be applied to the flexible body. The main constraint is the addition of a fixing sub at the right end of the earth and the fruit-bearing branch. The contact collision force between the fruit-bearing branch and the vibrating rod and the tooth comb plate is also added.

(2) Application of loads: The positive pressure and friction from the vibrating rod on the hanging branch, and the positive pressure and friction from the tooth comb plate on the fruit-bearing branch, cause the branch to vibrate. During the simulation, the *C. oleifera* fruit vibrates, collides and is combed by the vibrating rod and the tooth comb plate. Contact forces therefore need to be applied between the branch and the vibrating plate, and between the branch and the tooth comb plate.

(3) Establishment of a rigid-flexible coupling model: As shown in the figure below, we import the established 3D model of the device and branch into ADAMS software. We then import the fruit-bearing branch and change the previously created branch from a rigid body to a flexible one by clicking on the option *Create a flexible body* through the interface in the ADAMS flexible body module. Using the picking actuator as a reference, we adjust the position of the branch and use the movement and rotation functions in the ADAMS software to bring the flexible branch into contact with the picking actuator, as shown in Figure 6.

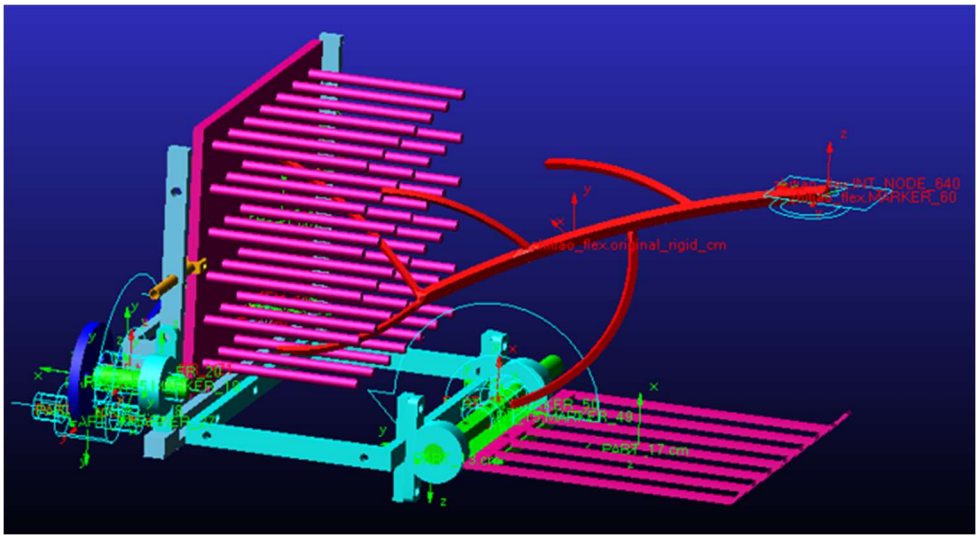

FIGURE 6. Rigid-flexible coupling model of the device and fruit-bearing branch.

(4) The inherent frequency of the system, based on the (Wu et al., 2021a) established *C. oleifera* fruit-branch vibration system, is around 7 Hz. The parameter settings used for the simulation and the analysis of results are as follows. When the picking actuators work together, the designed vibration frequencies are 3, 5 and 7 Hz, the amplitude is 80 mm, the tooth comb spacing is 35 mm, and the rotation speed of the tooth comb is 0.1 rad/s. Under these operating parameters, the vibration and combing operations of the picking actuators on the structural branch are used to analyze the speed, acceleration and force curve for the fruit-bearing branch, and to investigate the effect of the picking actuators on the fruit-bearing branch under these operating conditions. The simulation time was 3 s, and the number of steps was 500. The results are shown below, and the specific parameters are given in Table 2.

TABLE 2. Statistics for the simulation results.

Comb rotation speed rad/s	Vibration frequency /Hz	Branches					
		Maximum velocity mm/s	Average velocity mm/s	Maximum acceleration mm/s	Average acceleration mm/s	Maximum collision force N	Average collision force N
0.1	3	574.61	187.83	3.3106E+08	1.6303E+06	1558.28	55.70
	5	755.61	309.64	2.8844E+08	1.7007E+06	2700.30	82.72
	7	1095.80	436.98	1.9934E+08	1.4693E+06	3084.94	112.12

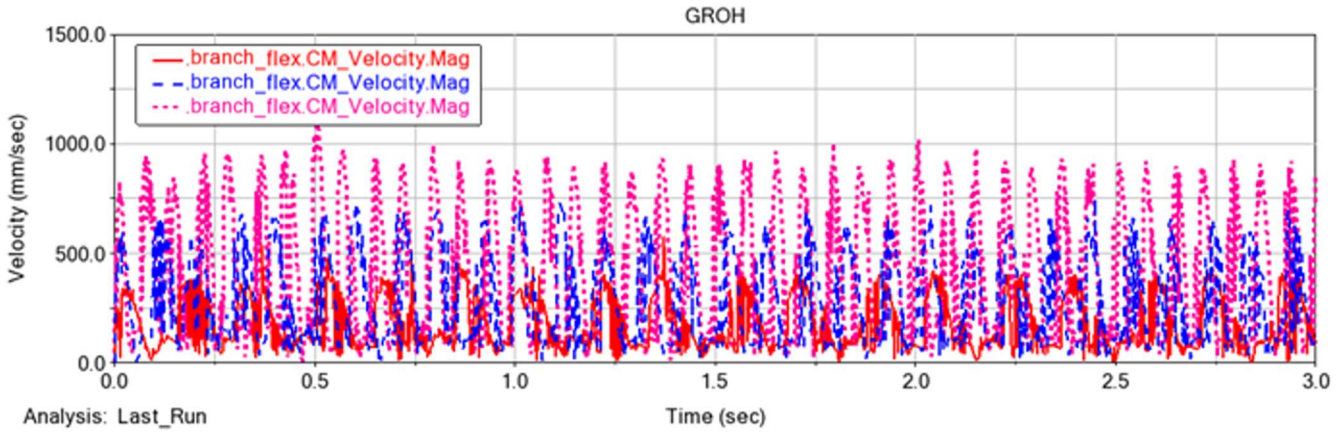

FIGURE 7. Speed curves for the fruiting branch under different operating parameters.

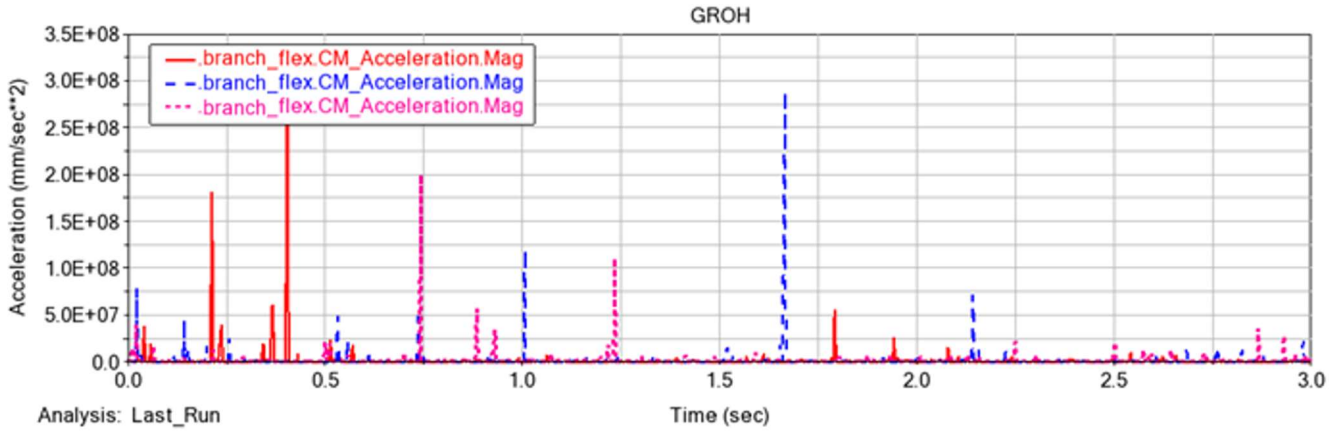

FIGURE 8. Results for the branch acceleration curve under different operating parameters.

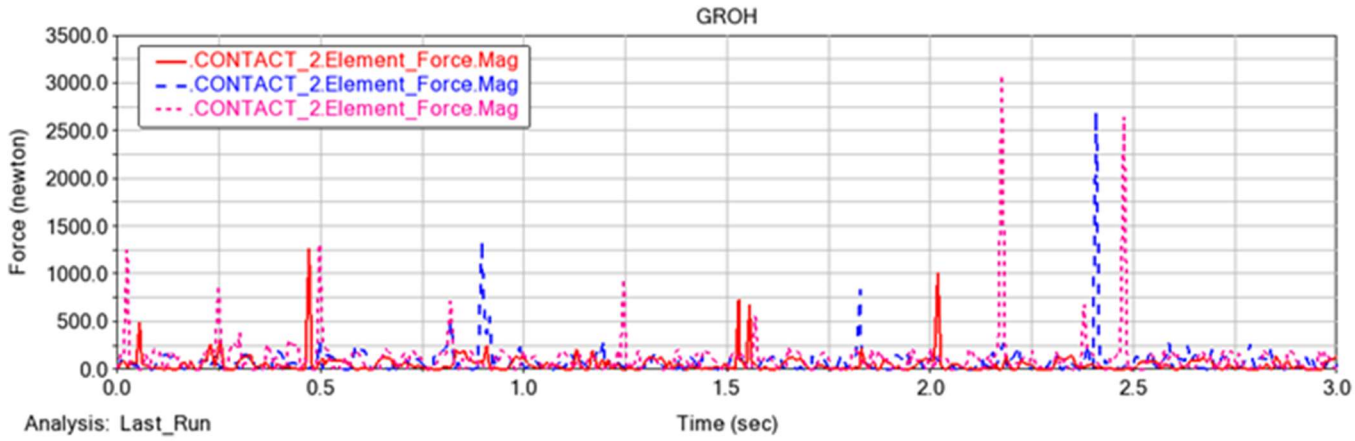

FIGURE 9. Collision force curves for the fruiting branch against vibrating plates at different frequencies.

From Figures 7, 8 and 9, which show the velocity and acceleration curves for the branch, it can be seen that the velocity of the branch varies significantly at different vibration frequencies, and that the average velocity of the fruiting branches is greatest at 7 Hz and least at 3 Hz. It can also be observed that as the vibration frequency of the vibrating plate increases, the velocity of the fruiting branches gradually increases, and the average velocity reaches a maximum at 7 Hz. The operating parameters used in the simulation can therefore be used as a direct reference for the operating parameters of the field trials.

According to Figure 9, the contact collision force between the fruiting branch and the vibrating plate changes when the branch is subjected to different frequencies of vibration. As the vibration frequency of the vibrating plate increases, the contact collision force between the fruiting branch and the vibrating plate gradually increases, and the average speed reaches a maximum at 7 Hz. The greater the contact collision force, the easier it is for the *C. oleifera* fruit to fall off, but at the same time, the damage to the hanging

fruit branches and buds increases; this means that a higher vibration frequency for the picking actuator is not better, and that appropriate parameters for the picking operation should be found. When the vibration frequency is 5 Hz, the average value of the contact collision force on the hanging branch is 82.72 N, which fully satisfies the conditions for shedding of the *C. oleifera* fruit.

Experiments on Picking Performance

In October 2021, tests of the performance of the proposed device were conducted at the forest bases of QingLongWan Agricultural Ecological Development Co., Ltd., in TongCheng City, and the Trap Nai Farm, Anhui Province, on eight-year-old ChangLin 4 *C. oleifera* trees. The field trials were conducted during the period when the fruit was ripe for harvesting.

FIGURE 10. Photograph of the picking process.

Since *C. oleifera* flowers and fruits at the same time, the fruit reaches maturity while flower buds are opening, and the number of flower buds will affect the yield in the following year. Hence, the fruit drop rate and flower loss rate from the plants were used as evaluation indicators. Before the trial, the initial numbers of fruits N_1 and the flower buds N_2 in the working space were counted, and after the trial, the final numbers of fruits N_3 and the flower buds N_4 in the working space were counted again.

The fruit drop rate P was calculated using the formula:

$$P = \frac{N_1 + N_2}{N_1} \times 100\% \tag{26}$$

while the flower loss rate Q was calculated as:

$$Q = \frac{N_2 + N_4}{N_2} \times 100\% \tag{27}$$

For the proposed fruit picking device, the rates of fruit drop and flower loss were used as evaluation indices for the test, and we varied three parameters, namely the vibration frequency A (Hz), the amplitude B (mm) of the vibrating plate, and the tooth comb spacing C (mm) of the tooth comb plate. Based on the results of this analysis, a Box-Behnken test was designed to investigate the effects of these different parameters on the picking effect and to determine the best combination (He et al., 2020).

Factor Level Test

In order to verify the efficacy of the proposed *C. oleifera* fruit picking device in actual operation, and to analyze the influence of various factors on the fruit drop and flower loss rates under different parameter combinations, the vibration frequency and amplitude of the vibrating plate and the tooth comb spacing of the tooth comb plate were selected as the test factors. The range of vibration frequency for the vibrating plate was 3–7 Hz, the amplitude was varied in the range 40–80 mm, and the tooth comb plate spacing was taken as 25, 35 and 45 mm. A three-factor, three-level orthogonal test was conducted on the fruit picking results of our device, and the factor levels are shown in Table 3.

TABLE 3. Test factor codes.

Level	A	B	C
1	7	80	45
0	5	60	35
−1	3	40	25

RESULTS AND DISCUSSION

A regression analysis of the process test results on *C. oleifera* fruits was carried out using Design-Expert 13.0.1 data analysis software, and the results for the significance of the effect of each factor on the fruit drop and flower loss rates are shown in Table 4. A quadratic polynomial response regression model was established between the fruit drop rate and flower loss rate and the vibration frequency A, amplitude B and tooth comb spacing C of the *C. oleifera* canopy.

TABLE 4. Experimental design options and results.

Test no.	Vibrating plate frequency (Hz)	Vibrating plate amplitude (mm)	Tooth comb plate spacing (mm)	Fruit drop rate (%)	Flower loss rate (%)
1	5	40	45	77.78	7.14
2	7	60	45	91.67	11.11
3	3	40	35	65.71	7.41
4	3	80	35	80.00	10.34
5	5	80	25	88.24	20.00
6	5	60	35	86.67	10.34
7	7	40	35	89.29	13.51
8	5	60	35	85.29	9.09
9	5	60	35	85.71	9.68
10	5	80	45	86.21	9.09
11	5	60	35	85.19	9.68
12	3	60	25	76.67	8.00
13	3	60	45	70.00	6.25
14	5	60	35	86.67	9.09
15	7	80	35	96.88	23.08
16	7	60	25	93.75	14.29
17	5	40	25	82.76	11.54

TABLE 5. Quadratic regression analysis of variance for fruit drop rate in *C. oleifera.*

Source	Sum of squares	df	Mean square	F-value	p-value
Model	1020.58	9	113.40	73.62	< 0.0001
A-A	784.28	1	784.28	509.18	< 0.0001
B-B	160.12	1	160.12	103.95	< 0.0001
C-C	31.05	1	31.05	20.16	0.0028
AB	11.22	1	11.22	7.29	0.0307
AC	5.27	1	5.27	3.42	0.1069
BC	2.18	1	2.18	1.41	0.2734
A^2	14.11	1	14.11	9.16	0.0192
B^2	5.15	1	5.15	3.34	0.1103
C^2	4.67	1	4.67	3.03	0.1252
Residual	10.78	7	1.54		
Lack of fit	8.68	3	2.89	5.52	0.0662
Pure error	2.10	4	0.5245		
Cor. total	1031.36	16			

TABLE 6. Quadratic regression analysis of variance for flower loss in *C. oleifera.*

Source	Sum of squares	df	Mean square	F-value	p-value
Model	294.64	9	32.74	10.47	0.0027
A-A	111.60	1	111.60	35.71	0.0006
B-B	64.07	1	64.07	20.50	0.0027
C-C	50.40	1	50.40	16.13	0.0051
AB	11.02	1	11.02	3.53	0.1025
AC	0.5929	1	0.5929	0.1897	0.6763
BC	11.49	1	11.49	3.68	0.0967
A^2	3.74	1	3.74	1.20	0.3104
B^2	39.61	1	39.61	12.67	0.0092
C^2	1.69	1	1.69	0.5398	0.4864
Residual	21.88	7	3.13		
Lack of fit	20.80	3	6.93	25.73	0.0045
Pure error	1.08	4	0.2694		
Cor. total	316.52	16			

Based on the data from the experimental analysis in Tables 5 and 6, a quadratic regression ANOVA was performed on the test results, using Design-Expert 13.0.1 software, and the fit coefficients were obtained to give a quadratic polynomial regression equation for the response values and independent variables. The quadratic regression model was highly significant (P<0.01), and the quadratic regression equation for the fruit drop rate of *C. oleifera* was obtained as follows:

$$Y_1 = 85.91 + 9.09A + 4.47B - 1.97C - 1.68AB + 1.15AC + 0.7375BC - 1.83A^2 - 1.11B^2 - 1.05C^2 \quad (28)$$

The quadratic regression equation for the flower loss rate of *C. oleifera* was obtained as follows:

$$Y_2 = 9.58 + 3.37A + 2.83B - 2.51C + 1.66AB - 0.3850AC - 1.7BC + 0.9420A^2 + 3.07B^2 - 0.6330C^2 \quad (29)$$

in which

Y_1 - fruit drop rate of *C. oleifera*, %;

Y_2 - rate of flower loss of *C. oleifera*, %.

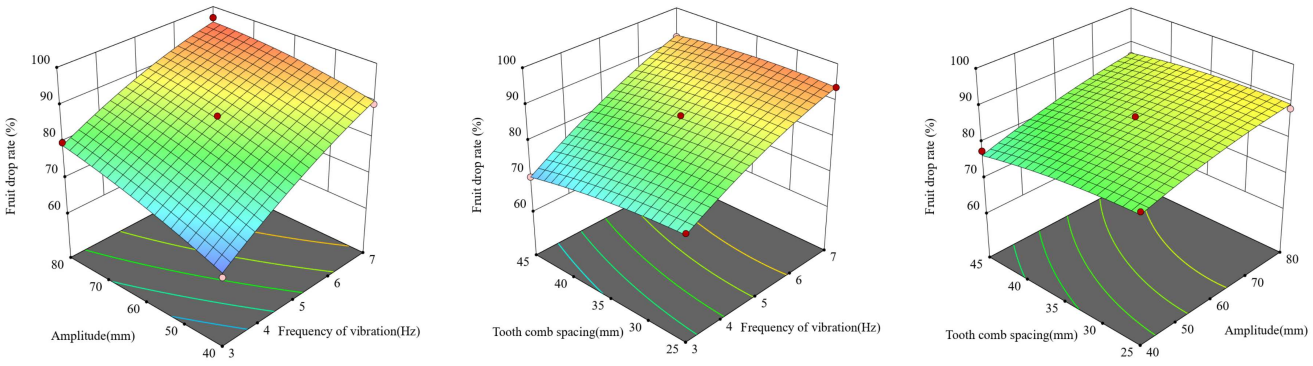

(a) Y_1= (A, B, 35) (b) Y_1= (A, 60, C) (c) Y_1= (5, B, C)

FIGURE 11. Response surface for the influence of each factor on the fruit drop rate in *C. oleifera.*

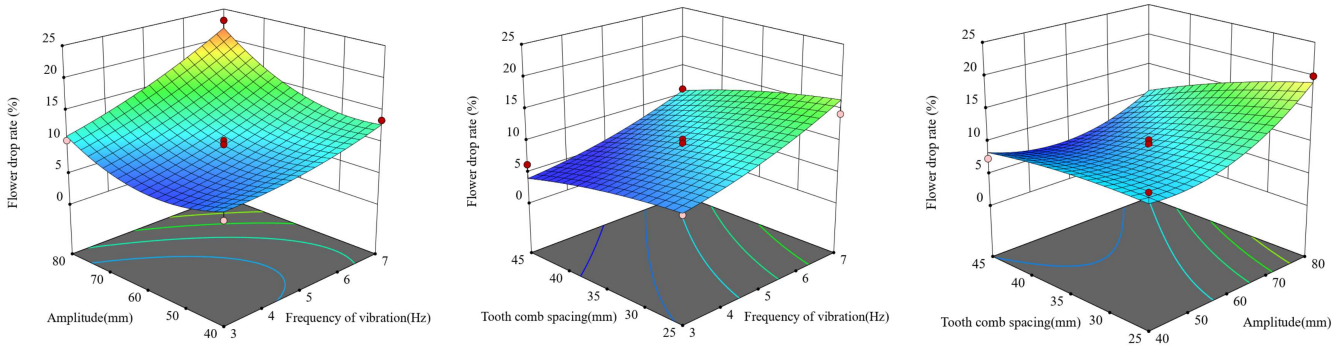

(a) Y_2= (A, B, 35) (b) Y_2= (A, 60, C) (c) Y_2= (5, B, C)

FIGURE 12. Response surface for the influence of each factor on the flower damage rate in *C. oleifera.*

Figure 11 and 12 show the response surface curves for each factor. In order to ensure a certain rate of fruit drop with the minimum rate of flower loss, the test results were optimized using Design-Expert 13.0.1 software, resulting in a set of 18 optimal picking parameter combinations. To achieve the lowest rate of flower loss, the vibration frequency was 5.85 Hz, the amplitude was 60.43 mm, and the tooth comb spacing was 45 mm. Under these conditions, the rate of fruit drop was 87.32% and the rate of flower loss was 8.06%.

Based on the above results, it can be concluded that the proposed vibration-comb brush *C. oleifera* fruit picking device gives good picking results. Compared to previous schemes (Wu et al., 2022, Gao et al., 2019), it has several advantages. (i) It has a lightweight design and simple structure, meaning that it has a low cost and is suitable for plantations at various scales. Existing harvesters give high-quality results but require a large amount of driving power, resulting in significant noise pollution. However, the mobile device presented here requires only one person to perform a simple dragging motion to complete the picking operation, making it suitable for flat or sloping *C. oleifera* plantations. (ii) The advantage of using two harvesting modes simultaneously lies in improved harvesting efficiency. The vibrating plate picks the outer layers of the fruit, while the toothed comb plate picks the inner layers, making picking more efficient. (iii) Our device has a low vibration frequency, thereby creating minimal damage and saving power, while effectively reducing damage to the branches of the trees.

However, the harvesting efficiency is reduced by 5% compared to existing devices. The main reason for this is the need for optimization in terms of the minimum flower drop rate, as a low flower loss during the picking period can ensure that next year's fruit yield is maintained, so the current harvesting efficiency has reached the production efficiency standard. Although the maximum possible harvesting efficiency of the device is around 95%, the flower damage rate under this configuration far exceeds the maximum allowable range of 10%, so it is not advisable. The vibration frequency obtained in this study as a suitable value for the device is only 5.85 Hz; this low vibration frequency and amplitude cause less damage to the tree during the picking process, making the device suitable for further development for the *C. oleifera* industry.

CONCLUSIONS

(1) A device based on a combination of vibration and brushing techniques for the harvesting of *C. oleifera* fruit was proposed. Mechanized picking of the fruits is achieved through the collaborative operation of external vibration, collision, and a rotary comb brush inside the canopy, meaning that the picking device exerts multiple forms of action on the fruits at the same time to promote the shedding of fruits.

(2) Using ADAMS software carried out kinematic and dynamic simulation analyses of the operation process of the picking actuator , and a rigid flexible coupling model of the proposed device was established. The picking actuator was moved to a branch with hanging fruit by applying a driving force to the vibration mechanism and the brush mechanism and the contact force between the picking actuator and the fruit. Through the ADAMS/AUTOFLEX module, a flexible model of the fruit-bearing branch was established, and a rigid flexible coupling simulation analysis was carried out. The speed, acceleration, collision force and other curves were calculated for the fruiting branch when the force had been obtained. A kinematics and dynamics analysis of the fruit-bearing branch can provide an important reference for analysis of the fall-off of *C. oleifera* fruit.

(3) A prototype device based on our vibration-comb-brush design for *C. oleifera* fruit was developed, and field tests were conducted. The fruit drop and flower loss rates after picking were used as experimental indicators, and through a three-factor and three-level orthogonal experiment, it was found that the vibration frequency of the vibration plate had the greatest impact on the fruit drop rate, followed by the vibration amplitude, and finally the tooth comb spacing. While aiming to ensure a certain fruit drop rate, the minimum flower loss rate was found. The optimal combination of parameters was as follows: vibration frequency 5.85 Hz, amplitude 60.43 mm, and tooth comb spacing 45 mm. Under these operating conditions, the highest fruit drop rate and the lowest flower loss rate were achieved. The fruit drop rate was 87.32%, and the flower loss rate was 8.06%.

ACKNOWLEDGMENTS

Thanks are also due to the editors and anonymous reviewers for their constructive suggestions for the paper.

FUNDING

The authors gratefully appreciate the Natural Science Foundation of Anhui Province (NO.2208085ME132).

REFERENCES

Du YW, Cheng JY, Yao XH, Deng XZ, Cheng YM, Wei ZY (2022) Comprehensive evaluation on picking efficiency of Camellia Oleifera clones fruits based on their canopy distribution and characteristics differences. Subtropical Plant Science 51(03):191-197. https://doi.org/10.3969/j.issn.1009-7791.2022.03.005

Fu QK, Fu J, Chen Z, Ren LQ (2020) Loss reduction mechanism and experiment on snapping of rigid-flexible coupling corn head. Journal of Agricultural Machinery 50(04): 60-68. https://doi.org/10.6041/j.issn.1000-1298.2020.04.007

Gao ZC, Li LJ, Li X, Min SH, Yi CF (2013) Development and test of picking actor in oil-tea camellia fruit picking machine of tooth comb type. Transactions of the Chinese Society of Agricultural Engineering 29(10): 19-25. https://doi.org/10.3969/j.issn.1002-6819.2013.10.003

Gao ZC, Zhao KJ, Li LJ, Pang GY, Wang XC (2019) Design and experiment of suspended vibratory actuator for picking Camellia Oleifera fruits. Transactions of the Chinese Society of Agricultural Engineering 35(21): 9-17. https://doi.org/10.11975/j.issn.1002-6819.2019.21.002

Hayashi S, Yamamoto S, Tsubota S, Ochiai Y, Kobayashi K, Kamata J, Kurita M, Inazumi H, Peter R (2014) Automation technologies for strawberry harvesting and packing operations in japan 1. Journal of Berry Research 4(1): 19-27. https://doi.org/10.3233/JBR-140065

He XY, Wang PZ, Li M, Song WT (2020) Parameters optimization of greenhouse air-cooled condenser heat collection and release system by response surface method. Journal of Agricultural Machinery 51(12):315-323.

He Z, Ma L, Wang YC, Wei YC, Ding XT, Li K and Cui YJ (2022) Double-arm cooperation and implementing for harvesting kiwifruit. Agriculture 12(11): 1763. https://doi.org/10.3390/agriculture12111763

Li C, Xing JJ, Xu LM, He SL, Li SJ (2015) Design and experiment of wine grape threshing mechanism with flexible combing striping monomer. Transactions of the Chinese Society of Agricultural Engineering 31(6): 290-296. https://doi.org/10.3969/j.issn.1002-6819.2015.06.040

Luo ST, Rao HF, Zhang LY, Yu JJ, Xu HQ, Li T, Liu MH (2017) Design and experiment of a tooth comb paddle knife type *Camellia oleifera* fruit picking device. Agricultural Mechanization Research 39(02): 84-88+157. https://doi.org/10.13427/j.cnki.njyi.2017.02.018

Rao HH, Zhang LY, Huang DS, Chen B, Liu MH (2018) Design and test of motor-driven picking actuator of Camellia fruit with rotate rubber roller. Journal of Agricultural Machinery 49(09): 115-121. https://doi.org/10.6041/j.issn.1000-1298.2018.09.013

Wang D, Tang JY, Fan ZY, Kou X, Qu ZJ (2020) Design and test of a vibratory Camellia Oleifera fruit harvester. Forestry Machinery and Woodworking Equipment 48(06): 4-7+14. https://doi.org/10.13279/j.cnki.fmwe.2020.0061

Wu DL, Yuan JH, Li C, Jang S, Ding D, Cao CM (2021b) Design and experiment of twist-comb end effector for picking Camellia fruit. Journal of Agricultural Machinery 52(04): 21-33. https://doi.org/10.6041/j.issn.1000-1298.2021.04.002

Wu DL, Zhao EL, Jiang S, Da D, Liu YY (2022) Influence of excitation position on mechanized picking effect of Camellia Oleifera. Engenharia Agrícola 42(4): e20220040. https://doi.org/10.1590/1809-4430-Eng.Agric.v42n4e20220040/2022

Wu DL, Zhao EL, Jiang S, Ding D, Liu YY, Liu L (2021a) Optimization analysis and test of canopy vibration parameters of Camellia fruit based on double pendulum model. Journal of Agricultural Machinery 52(12): 96-104. https://doi.org/10.6041/j.issn.1000-1298.2021.12.010

Yu YJ, Wang J, Lai QH, Jia QH, Yu F, Cao Y (2021) Design and experiment of hand-held vibrating comb-type Coffea arabica L. Journal of Agricultural Machinery 52(09):124-133.

Yu YJ, Ying C, Lai QH, Zhao QH, Sun ZX, Zhou SW, Song DK (2023) Design and operation parameters of vibrating harvester for Coffea arabica L. Agriculture 13(3): 700. https://doi.org/10.3390/agriculture13030700

Zhang WQ, Zhang MM, Zhang JX, Li W (2018) Design and experiment of vibrating wolfberry harvester. Journal of Agricultural Machinery 49(7): 97-102. https://doi.org/10.6041/j.issn.1000-1298.2018.07.012

Zhu L, Wang S, Wan F, Zhou Y, Wang Z, Fan G, Wang P, Luo H, Liao S, He L, Yang Y, Li X, Zou X, Chen S, Zhang J (2023) Quantitative analysis of Camellia Oleifera seed saponins and aqueous two-phase extraction and separation. Molecules 28(5):2132. https://doi.org/10.3390/molecules28052132